Property and Shape Modulation of Carbon Fibers Using Lasers

Blaker, Jonny; Anthony, David; Tang, Guang; Shamsuddin, Siti-Rose; Kalinka, Gerhard; Weinrich, Malte

Published in:
ACS Applied Materials & Interfaces

DOI:
10.1021/acsami.6b05228

Publication date:
2016

Document Version
Peer reviewed version

Property and Shape Modulation of Carbon Fibers Using Lasers

Jonny J. Blaker[1*], David B. Anthony[2,3], Guang Tang[4], Siti-Ros Shamsuddin[3], Gerhard Kalinka[5], Malte Weinrich[5], Amin Abdolvand[4], Milo S. P. Shaffer[2] and Alexander Bismarck[3,6]

[1] Bio-/Active Materials Group, School of Materials, MSS Tower, The University of Manchester, M13 9PL, United Kingdom

[2] Nanostructured Hierarchical Assemblies and Composites Group (NanoHAC), Department of Chemistry, Imperial College London, South Kensington Campus, London, SW7 2AZ, United Kingdom

[3] Polymer and Composite Engineering (PaCE) Group, Department of Chemical Engineering, Imperial College London, South Kensington Campus, London, SW7 2AZ, United Kingdom

[4] Materials & Photonics Systems (MAPS) Group, School of Science and Engineering, University of Dundee, Dundee DD1 4HN, United Kingdom

[5] BAM Federal Institute for Materials Research and Testing, Berlin, Germany

[6] Polymer and Composite Engineering (PaCE) Group, Institute of Materials Chemistry and Research, Faculty of Chemistry, University of Vienna, Währinger Str. 42, A-1090 Vienna, Austria

Corresponding Author

*Email: jonny.blaker@manchester.ac.uk

Abstract

An exciting challenge is to create unduloid-reinforcing fibers with tailored dimensions to produce synthetic composites with improved toughness and increased ductility. Continuous carbon fibers, the state-of-the-art reinforcement for structural composites, were modified via controlled laser irradiation to result in expanded outwardly tapered regions, as well as fibers with Q-tip (cotton-bud) end shapes. A pulsed laser treatment was used to introduce damage at the single carbon fiber level, creating expanded regions at predetermined points along the lengths of continuous carbon fibers, whilst maintaining much of their stiffness. The range of produced shapes was quantified and correlated to single fiber tensile properties. Mapped Raman spectroscopy was used to elucidate the local compositional and structural changes. Irradiation conditions were adjusted to create a swollen weakened region, such that fiber failure occurred in the laser treated region producing two fiber ends with outwardly tapered ends. Upon loading the tapered fibers allow for viscoelastic energy dissipation during fiber pull-out by enhanced friction as the fibers plough through a matrix. In these tapered fibers, diameters were locally increased up to 53%, forming outward taper angles of up to 1.8°. The tensile strength and strain to failure of the modified fibers were significantly reduced, by 75% and 55%, respectively, ensuring localization of the break in the expanded region; however, the fiber stiffness was only reduced by 17%. Using harsher irradiation conditions, carbon fibers were completely cut, resulting in cotton-bud fiber end shapes. Single fiber pull-out tests performed using these fibers revealed a 6.75 fold increase in work of pull-out compared to pristine carbon fibers. Controlled laser irradiation is a route to modify the shape of continuous carbon fibers along their lengths, as well as to cut them into controlled lengths leaving tapered or cotton-bud shapes.

1. Introduction

It remains challenging to produce unduloid carbon fibers, which can be expected to result in an increased pull out work, hopefully to realize new composites. The outward tapering and geometric dovetailing motifs observed in the reinforcement phase of nacre[1-3] have been successfully implemented in macro-composites[4] and more recently to 3 mm diameter short steel fibers with machined conical ends.[5] Fiber pull-out tests of these steel fibers from an epoxy matrix demonstrated that fibers with an taper angle of 5° dissipated up to 27 times more energy than straight fibers, whereas larger angles induced premature matrix failure.[5]A significant enhancement in work of pull-out and maximum pull-out force was also observed at 2° (circa 20 fold improvement).[5] The size of the enlarged fiber ends can alter the residual stress state producing either tensile or compressive tractions at the fiber interface.[6] Well-designed composites can undergo multiple fracture events, spreading fiber/matrix debonding and fiber pull-out across large volumes, allowing significant deformation before a crack localizes and the composite fails.[7] Tapered fibers can bridge cracks and plough through the matrix, contributing to viscoplastic energy dissipation. There is a growing body of evidence from synthetic composite materials,[6,8-12] which shows that suitably bulbous/tapered fiber ends and wavy fibers[13,14] can act to increase the work of pull-out, delocalize inelastic deformation and induce strain-hardening. Fabrication routes include thermal deformation, as applied to thermoplastic UHMWPE (Dyneema™) fibers,[8] fiber knotting,[9] and mechanical deformation to result in wavy or flat-ended fibers.[9-12] It is a significant challenge to transpose outward tapering features and an unduloid fiber shape to continuous carbon fibers, the preferred reinforcements in high performance composites, with typical diameters in the range 5-10 μm. Short 'cotton-bud' carbon fibers might be applied as short fiber reinforcements. More ideally, the

fibers would break, *in situ*, to form the tapered segments, since continuous fibers can be more readily processed into high loading fraction, aligned composites and would provide higher initial stiffness.

Lasers are being increasingly applied to cut holes and shapes into high performance unidirectional (UD) carbon fiber composites,[15-21] as well as to perforate laminates, cutting fibers at predefined points to produce highly aligned discontinuous composites mainly with the aim to improve manufacturing ductility.[22,23] Carbon fibers cut via laser ablation have been reported to feature expanded ends (up to 60%) in the vicinity of the heat-affected zones of such laser-drilled holes.[17,22-24] This local expansion has been attributed to irreversible changes in the arrangements of the basal planes, caused by rapid heating and steep thermal gradients occurring during laser cutting, volatising non-carbon impurities within the structure of the fibers.[15,16] Controlled laser irradiation therefore presents an opportunity to modify the shape of continuous carbon fibers along their lengths.

The current work systematically investigates the effect of laser treatment on single carbon fibers to produce i) continuous fibers with expanded regions, ii) continuous fibers with expanded and ablated (necked) regions, and iii) ablated fibers with expanded, i.e. cotton-bud shaped, fiber ends. The mechanical properties of the treated continuous fibers are evaluated by single fiber tensile testing and their failure points assessed post-mortem. Laser mapping Raman spectroscopy is used to elucidate compositional and structural changes due to laser irradiation. The pull-out response of the ablated, cotton-bud end fibers is investigated by single fiber pull-out tests.

2. Experimental section

2.1 Materials

Unsized, polyacrylonitrile (PAN) based AS4 carbon fibers were kindly provided by Hexcel Ltd. (Cambridge, UK). According to the manufacturer the AS4 fibers have a carbon content of 94%, tensile modulus of 230 GPa, tensile strength 4430 MPa, and elongation at break of 1.8%. Two-part epoxy adhesive, Araldite® Rapid Adhesive was used to glue single carbon fibers to paper frames, which acted as temporary supports for testing. The conductive paint used for scanning electron microscopy (SEM) was Acheson Silver DAG 1415 M (Agar Scientific, UK). The matrix material chosen for single fiber pull-out tests was a two-component pourable transparent silicone rubber, Elastosil® LR 7665 A/B (Wacker Chemie AG, München, Germany). Elemental analysis performed on unsized AS4 fibers confirmed that the fibers have a carbon content of 94.72%, with nitrogen, oxygen, hydrogen and sulphur contents of 4.62%, 0.2%, 0.12% and <0.02%, respectively.

2.2 Carbon Fiber Mounting for Laser Irradiation

Single fibers were individually fixed on white paper frames (80 gsm) using epoxy adhesive and end-tabbed with paper. These frames allowed for positioning and handling of the fibers for laser irradiation (depicted in Figure 1) as well as scanning electron microscope (SEM) evaluation, Raman spectroscopy, single fiber tensile testing (gauge length 20 mm) and post-failure SEM analysis. Small scalpel cuts were made on the paper frames in line with the centre of the gauge length, serving as guides to position the fibers for irradiation and location of the modified region for SEM and Raman spectroscopy.

2.3 Laser Irradiation to Effect Fiber Shape Change and Local Weakening

Frames containing the fibers were mounted on anodized aluminium substrates using thin strips of 3M Magic tape to maintain the fibers flat. The substrates were positioned underneath the laser beam, such that the laser guide path would run vertically through the length of a single column, to irradiate through the mid section of 10 fibers at a time. A nanosecond (8 ns) pulsed Nd: YVO_4 laser with a maximum average power of 17.5 W at λ = 1064 nm was operated with parameters in the range of 1.1 - 17.5 W of average power, a repetition rate in the range of 50 - 100 kHz and beam scanning speeds in the range of 50 - 200 mm s^{-1}. The laser beam was focused to a spot size of ~ 70 μm in diameter on the target. The laser had a Gaussian profile and the focal point was set to the height of the substrate in an effort to irradiate all fibers equally. Laser conditions were adjusted and resulted in three different fiber shapes (Figure 1), causing (i) local expansion of the fiber at the irradiation site, (ii) expansion and ablation of the fibers, and (iii) expansion and cutting of the fibers. These fiber classes are called Expanded, Expanded/Ablated and Cotton-bud end fibers, respectively (Figure 1). Laser parameters 1.1 W of average output power, frequency 100 kHz, and speed 100 mm s^{-1} resulted in ca. 20% of fibers being cut; at 17.5 W, frequency 50 kHz and speed 50 mm s^{-1} all fibers were cut. Parameters 1.1 W, frequency 100 kHz and speed 200 mm s^{-1} consistently resulted in intact fibers. Immediately post irradiation, the fibers were investigated using a digital microscope surface profiling system (KEYENCE VHX-1000) to confirm the effect of irradiation conditions on fiber morphology and fiber cutting. The laser operated at 1.1 W of average power had an energy fluence of 0.3 J cm^{-2} (energy per pulse 11 μJ). The laser fired 35 pules per spot, since the laser was run at 100 kHz and speed 200 mm s^{-1}. 1D temperature modelling has been conducted for this condition. A rough estimate shows

that the temperature rise in the focus of the beam during the processing is in excess of 2900 K. The vaporization temperature of PAN-based carbon fibers is reported[15] to be 3500 K and the axial thermal conductivity 6.83 W m^{-1} K^{-1}, as reported by the manufacturer. For the same average power, when lower scanning speeds, such as 100 mm s^{-1} or 50 mm s^{-1}, were used there are 70 and 140 pulses per spot, respectively, leading to cutting of the fibers. When higher average powers were used (17.5 W) the fibers were also cut due to temperature in excess of carbon vaporization. The effect of laser treatment on the mechanical properties of Expanded and Expanded/Ablated fibers, compared to Control carbon fibers was assessed via single fiber tensile testing. Single fiber pull-out tests were conducted on Cotton-bud end carbon fibers to assess enhancement of pull-out behaviour due to shape modification in comparison to control carbon fibers.

2.4 Quantification of Fiber Shape Modification

SEM was conducted on individual irradiated and control fibers mounted in paper frames using a JEOL 5160 LV SEM (Jeol Ltd., Japan). The end tab region of the paper frames were attached to SEM stubs via adhesive carbon tabs. A small amount of conductive silver paint was added to the end of the tab, to connect the carbon fiber to the holder. Care was taken not to allow the carbon fibers to directly touch the adhesive carbon tab in order to keep the fibers in tact. This technique allowed the same irradiated fiber to be imaged prior and post tensile testing to assess the fiber shape after irradiation/ablation and to determine the failure point, respectively. A scalpel blade was used to carefully remove the paper templates from the adhesive carbon tab ahead of tensile testing. The software ImageJ (Version 1.48, NIH, USA) was used to quantify fiber shape modification (Figure 1). The affected length is

defined here as the region with a diameter in excess of 0.1 μm of the unaffected region. The apparent taper angle θ of the expanded fibers was determined using Equation 1:

$$\theta = \tan^{-1} \frac{(d_{max} - d_0)}{2L} \qquad \text{Equation 1}$$

where d_{max} is the maximum expanded diameter, d_0 the fiber diameter of the unaffected region, and L the affected length (θ represents the angle formed at one side of the fiber only). Irradiated regions were also investigated using high-resolution field emission gun scanning electron microscope (FEG-SEM) (Leo Gemini 1525 using SmartSEM software interface V05.05.03.00, 2010, Carl Zeiss NTS Ltd., UK). Quantitative measurements are based on 30 fibers with standard errors provided.

2.5 Single Fiber Tensile Testing

Expanded and Expanded/Ablated single carbon fibers were tensile tested at 21 °C with a crosshead speed of 15 μm s^{-1} following BS ISO 11566:1996 using a TST 350 tensile testing rig (Linkam Scientific Instrument Ltd., UK) equipped with a 20 N load cell. The paper end tabs were gripped in the machine and then the lateral parts of the frames cut through using fine scissors allowing the fiber to be loaded. The displacement and load were recorded, and later converted to stress and strain. Tensile tests were conducted on a group of 30 carbon fibers.

2.6 Raman Spectroscopy of Control and Ablated Fiber Regions

Raman spectroscopy provides a non-destructive method of probing global properties of graphitic carbon materials by determining the D mode (1350 cm^{-1}), G mode (1582

cm^{-1}) and 2D mode (2700 cm^{-1}, overtone of the D mode).[25] Raman spectra were measured using a LabRAM Infinity system with 532 nm (2.33 eV) Nd-YAG green laser (numerical aperture (NA) 0.55/50x, maximum power 24 mW, LabSpec V4.18-06 2005 software interface, Horiba Jobin Yvon Ltd., UK) and on a Renishaw inVia micro-Raman spectrometer with 532 nm (2.33 eV) DPSS diode (NA 0.8/100x, sample power 3.2 mW, WiRE 4.1 HF7241 software 2014 interface, Renishaw PLC, UK) in backscattered geometry, with relative laser spot diameters 1.2 μm and 0.8 μm respectively, with a spatial resolution of ca. 1 μm in each system. Raman spectra were processed and Raman maps produced using WiRE software using spectra that were background subtracted and normalized with respect to the G mode. Intensity ratio maps for D mode/G mode (I_D/I_G) and 2D mode/G mode (I_{2D}/I_G) were sampled from 5-95% of total binned data to remove extremities and undesired weighting towards noise, which becomes significant. Raman I_D/I_G ratio and I_{2D}/I_G ratio intensity maps are also shown with a black mask to better display ratios since, outside the fiber cross-section noise dominated; the masks were generated from intensity D mode (I_D) maps, which accurately matched the optical images. Relative intensity G mode maps are normalised and are shown without masks.

2.7 Single Fiber Pull-out Testing

The apparent interfacial shear strength (τ_{IFSS}) and the work of pull-out were determined using single fiber pull-out tests. τ_{IFSS} is a measure of 'practical' adhesion between the fiber and matrix. In this test, a special transparent glass chamber was used to hold the matrix material. The fiber was attached to a steel screw using cyanoacrylate adhesive. The matrix used was Elastosil® LR 7665 A/B (Wacker), a

pourable, two-component compound liquid silicone rubber. The mixed uncured matrix was then poured into the glass chamber and the fiber embedded slowly into the matrix to an embedded length of ~200 μm. The matrix was then cured at 45 °C for 10 h in an oven, then removed and cooled to ambient temperature. Fiber pull-out tests were performed using a piezo-motor fixed on a stiff frame to avoid energy storage in the free fiber length between the matrix surface and clamping device. The fiber was loaded at a speed of 5 μm s^{-1} and pulled out of the matrix while the force was recorded throughout the experiment by a load cell. τ_{IFSS} was calculated from $\boldsymbol{F}_{\mathrm{MAX}}$ required to trigger de-bonding of the embedded carbon fiber from the matrix using Equation 2:

$$\tau_{IFFS} = \frac{F_{MAX}}{\pi d_f L} \qquad \text{Equation 2}$$

where d_f is the fiber diameter and L the embedded fiber length (determined from the load-displacement curves). The work of pull-out was determined by the area under the load-displacement curve. During the fiber pull-out process, images were captured using an optical microscope (Axionplan Zeiss equipped with an Axiocam ICc3 camera (Carl Zeiss Microscopy GmbH, Germany)) to assess the pull-out characteristics of the fibers with modified ends from the surrounding matrix.[26] Difficulties in sample preparation lead to only 5 control samples and 3 Cotton-bud end fibers being tested.

3. Results and Discussion

3.1 Effect of Laser Irradiation on Fiber Morphology and Shape

The laser treated fibers consistently exhibited an affected region along their length, consistent with a single pass of the laser. Three resulting fiber classes (Expanded, Expanded/Ablated and Cotton-bud end) were obtained depending on the focal point of the laser (Figure 1). The diameter of laser treated fibers increased from 7.0 μm, i.e. the average diameter of the control fibers, to a maximum of 9.7 μm, corresponding to an increase of 37% (Expanded fibers). The average affected length of these Expanded carbon fibers after a single laser pass was ~140 μm, resulting in a taper angle ~ 1°. Expanded/Ablated fibers exhibited slightly larger affected lengths with narrowed midsections, flanked by expanded regions, with taper angles of 1.6°. Cotton-bud end fibers were completely cut (ablated) through and had average affected lengths of 108 μm with taper angles of 1.8° (as detailed in Figure 1). The maximum expansion observed was 53%, after which ablation reduced the expanded fiber diameter, eventually cutting the fiber, resulting in characteristic Cotton-bud shaped fiber ends. This expansion value is comparable to those observed for PAN-based (T300) fibers in the perimeter of laser-drilled holes.[16] Voisey *et al.*[16] established that swelling up to 60% occurred when laser drilling low modulus T300 fibers, embedded in a PEEK matrix.[17] Interestingly, carbon fibers containing fewer impurities (higher C contents) were reported to be apparently less susceptible to laser-induced expansion in the perimeter of laser-drilled holes.[16]

3.2 Effect of Laser Ablation on Fiber Tensile Properties

The tensile properties of Expanded and Expanded/Ablated carbon fibers were significantly reduced in comparison to control AS4 fibers (Figure 2 (a-d)). All fibers exhibited a linear elastic behaviour with brittle fracture. The control carbon fibers failed catastrophically, breaking into fragments, whereas the laser treated fibers broke

into two, at their pre-defined weak point (expanded or ablated regions) resulting in outwardly tapered fiber ends (Figure 3) (for an Expanded carbon fiber). The fiber tensile strength (Figure 2 (b)) was significantly reduced at the laser-treated location, by ~69% for Expanded fibers, and 75% for Expanded/Ablated fibers. Modulus of laser treated fibers (Figure 2 (c)) were modestly reduced, by ca. 17% (averaged over all treated fibers) in comparison to the control fibers. The tensile strength and stiffness were calculated based on the cross-section of the original unmodified fiber, partly as not all the failed fiber ends could be recovered after testing but also because the relative performance compared to the original fiber is both easier to understand and more relevant to subsequent composite performance. Strain to failure of the laser treated fibers was significantly reduced, in line with the strength, (Figure 2 (d)) from 1.8% (Control fibers) to 0.6% (Expanded fibers), and 0.5% for Expanded/Ablated fibers. Whilst the local reduction in strength is quite significant, the effect is useful in the correct context. The fibers retain sufficient strength to be handled and potentially processed into high loading fraction composites, and the stiffness is broadly retained. A significant reduction in strength is, in fact, needed to localise the failure reliably at the desired, shaped location. Whilst the strength reduction is greater than required, the distribution of pre-weakened points can be designed to minimise the reduction in strength of the overall composite, by adjusting (proto)fragment aspect ratio and distribution.

3.3 Raman Spectroscopy and Mapping of Laser Treated Fibers

Raman analysis on the surface and in the interior (fracture surface) of the Control, Expanded and Expanded/Ablated carbon fiber morphologies provides information about the local degree of crystallinity (Figure 4 (a-f)). The Raman spectra of the

Control carbon fiber were very consistent along the whole fiber length and across the internal cross-section (Figure 4 (b) and (e)). The uniformity of relative I_G, I_D/I_G ratio and I_{2D}/I_G ratio can be clearly seen in individual Raman spectra (Figure 4 (e)) and more vividly in the Raman maps (Figure 4 (f)). The cross-section of the Control carbon fiber is regular and circular, typical for commercial grade carbon fibers. The absence of the 2D mode in the as-received AS4 fiber, a mode related to the 2nd order phonon scattering, can be attributed to the relatively low carbonization and graphitisation temperatures, c.a. 1300 °C, of PAN-derived high strength carbon fibers.[19] In the Expanded regions, the D and G modes sharpen and the 2D mode emerges, becoming more intense along the fiber axis towards the irradiated region (Figure 4 (a) and (b) from region 1 to 5). These changes indicate that the underlying carbon structure of the carbon fiber is more crystalline in the irradiated zone. Temperatures on the order of 2000 °C are easily achieved in laser irradiation (see section 2.3), leading to reordering of carbon structure in the PAN fiber turbostratic core. Raman maps of the Expanded fiber show an increased but comparatively uniform I_D/I_G intensity ratio over the cross-section, suggesting that the whole fiber has been modified in the irradiated region. Yet, the I_{2D}/I_G ratio in the cross-section indicates that the outer shell is most graphitized, presumably as it is heated most strongly (Figure 4 (f)). Although the remaining carbon is more graphitic, in the Expanded regions, the fiber surfaces are damaged; showing roughened and pitted morphology, with very slight increase in oxygen content (supplementary information, Figure S1). Expanded/Ablated carbon fibers show a similar trend along the modified region (Figure 4 (b)) flanked by regions, which were not laser irradiated. In the ablated cross-section ('C'), the graphitic shell is more obvious, consistent with the development of higher temperatures. Expanded and Expanded/Ablated fibers show a

distinctly non-circular cross-section attributed to the asymmetric laser illumination (Figure 4 (d)). The Raman mapping shows that laser treated fibers exhibit alterations to the core structure throughout the cross-section, as only hypothesized previously in literature.[16] It is clear that the tapered shape arises primarily from expansion and not from deposition of a distinct phase. This mechanism is preferable in the current context, as there is no weak interphase within the tapered region, which might lead to a premature shear failure. It is preferable that the jamming/wedging loads on the fiber end are transferred to the full fiber cross-section. As the cross-section increases, and some material may be ablated, the density in the modified region must decrease; on the other hand, the density of carbon should increase with increasing degree of graphitization. Since no pores are observed by SEM, there must be an increase in microporosity within the fiber due to thermal expansion/contraction effects and/or the evolution of volatiles. Expanded and Expanded/Ablated fibers show a distinctly non-circular cross-section understood to originate from the uneven modification caused by laser irradiation, with one side of the fiber witnessing greater energy absorption and subsequent expansion (or ablation) when compared to the non-irradiated side (Figure 4 (d)). Irregular cross-sectional profiles of the irradiated samples are unlikely to be a product of the single fiber tensile test, as carbon fibers fail in a brittle catastrophic manner. The increased degree of graphitization of the modified regions is consistent with the relative retention of stiffness but loss of strength, as observed for carbon fibers in general as a function of graphitization temperature; the presence of microporosity may magnify this trend.

3.4 Single Fiber Pull-out Tests

The pull-out behaviour of the cotton-bud terminated carbon fibers can be visualized by single fiber tests in a transparent silicone rubber matrix (Figure 5 (a) and (b)). Significant ploughing of the Cotton-bud end fibers through the matrix was evident and disruption of the matrix observed (Figure 5 (b)); in contrast, the Control fibers exhibited clean pull-out (Figure 5 (a)). The work of pull-out was found to increase dramatically, ~7 fold for cotton-bud end fibers, compared to Control carbon fibers (Figure 5 (c)). Normalized to embedded length this constitutes an improvement from 2.3 ± 0.6 μJ mm^{-1} for Control carbon fibers to 18.7 ± 3.6 μJ mm^{-1} for cotton-bud end fibers. The apparent interfacial shear strength for cotton-bud fibers improved ~5-fold compared to Control fibers. The intended wedging interaction is clearly demonstrated here, with taper angles of 1-2° being sufficient to cause cavitation in the matrix along with sliding. Whilst the optimum taper angle found for millimetre thick stainless steel fibers in epoxy was found to be 5°, carbon fibers are anisotropic and obtaining angles larger than those reported here remains a challenge. The transparent silicone matrix provides an easy way to visualize the load transfer and local deformation associated with the tapered ends over a long embedded length. Further studies with high stiffness structural matrices will be very helpful to understand the potential of the approach more fully. Semicrystalline thermoplastic matrices may be most effective in practice, although they tend to be opaque. On the other hand it is interesting to note that biological systems are often designed with a hard reinforcement and a very soft matrix.[1-3]

4. Conclusions

High power laser treatment can used to modify structural carbon fibers systematically, to create expanded, graphitized regions at predetermined points; the fiber strength was

locally reduced whilst much of their stiffness was retained. After treatment, the fibers consistently broke in the expanded regions, producing fiber segments with outwardly tapered ends having taper angles of 1-2°. The most effective laser parameters that result in laser treated carbon fibers remaining continuous with predefined break/weak points were with laser energy fluence of ~ 0.3 J cm^{-2} and beam scanning speed of 200 mm s^{-1} for this particular 1064 nm nanosecond pulsed laser system. More aggressive laser treatment - increasing the number of pulses fired per spot and/or increasing the laser energy fluence - led to the simultaneous expansion and ablation of the carbon fibers, eventually cutting them, to yield 'cotton-bud' fiber ends. Raman mapping demonstrated that the fiber structure was modified throughout the illuminated region, and that the expansion is due to intrinsic modification of the fiber structure. The laser-treated fibers possessed an increased crystallinity due to the high temperature evolved, with a greater effect at the fiber surface. The effectiveness of the laser treatment to modify pull-out characteristics was successfully demonstrated using 'cotton-bud' samples, which offer a significant ~7 fold increase in work of pull-out compared to control carbon fibers, without additional fiber failure. The results confirm a promising route to generate tapered carbon fibers, translating a key geometric feature of natural composites to the current state-of-the-art structural materials. Modified continuous carbon fibers could be used to form aligned high stiffness unidirectional composites with predefined (and distributed) weak regions. As fragmentation proceeds, a well-aligned short fiber composite will form, which retains the high modulus close to that of a unidirectional composite, but with shaped fragment ends that modulate subsequent fiber pull out. In both cases, the length of fiber fragments, fiber taper angle and nature of matrix will have to be optimized to

maximise both sliding and load transfer. Theory developed for other model systems[27-30] will offer helpful guidelines.

References

(1) Fratzl, P.; Weinkamer, R. Nature's Hierarchical Materials. *Prog. Polym. Sci.* **2007**, *52*, 1263-1334.

(2) Barthelat, F.; Tang, H.; Zavattieri, P.D.; Li, C-D.; Espinosa, H.D. On the Mechanics of Mother-of-pearl: A Key Feature in the Material Hierarchical Structure. *J. Mech. Phys. Solids* **2007**, *55*, 306-337.

(3) Rabiei, R.; Bekah, S.; Barthelat, F. Nacre from Mollusk Shells: Inspiration for High-performance Nanocomposites, Chapter 5, pp. 113-149, in RSC Green Chemistry No. 17 Natural Polymers, volume 2: Nanocomposites, Eds. John, M.J. and Thomas S., Pub. The Royal Society of Chemistry.

(4) Barthelat, F.; Zhu, D. A Novel Biomimetic Material Duplicating the Structure and Mechanics of Natural Nacre. *J. Mater. Res.* **2011**, *26*, 1203-1215.

(5) Humburg, H.; Zhu, D.; Bezina, S.; Barthelat, F. Bio-inspired Tapered Fibres for Composites with Superior Toughness. *Compos. Sci. Technol.* **2012**, *72*, 1012-1019.

(6) Beyerlein, I.J.; Zhu, Y.T.; Mahesh, S. On the Influence of Fiber Shape in Bone-Shaped Short-fibre Composites. *Compos. Sci. Technol.* **2001**, *61*, 1341-1357.

(7) Lin, Z.; Li, V.C. Crack Bridging in Fibre Reinforced Cementitious Composites with Slip-hardening Interfaces. *J. Mech. Phys. Solids* **1997**, *45*, 763-787.

(8) Zhu, Y.T.; Valdez, J.A.; Shi, N.; Lovatom, M.L.; Stout, M.G.; Zhou, S.J.; Butt, D.P.; Blumenthal, W.R.; Lowe, T.C. A Composite Reinforced with Bone-Shaped Short-fibres. *Scr. Mater.* **1998**, *38*, 1321-1325.

(9) Wetherhold, R.C.; Lee, F.K. Shaped Ductile Fibres to Improve the Toughness of Epoxy-matrix Composites. *Compos. Sci. Technol.* **2001**, *61*, 517-530.

(10) Bagwell, R.M.; McManaman, J.F.; Wetherhold, R.C. Short Shaped Copper Fibres in Epoxy Matrix: Their Role in a Multifunctional Composite. *Compos. Sci. Technol.* **2006**, *66*, 522-530.

(11) Bagwell, R.M.; Wetherhold, R.C. Fibre Pull-out Behaviour and Impact Toughness of Short Shaped Copper Fibres in Thermoset Matrices. *Composites, Part A* **2005**, *36*, 683-690.

(12) Bagwell, R.M.; Wetherhold, R.C. End-shaped Copper Fibers in an Epoxy Matrix – Predicted Versus Actual Fibre Toughening. *Theor. Appl. Fract. Mech.* **2005**, *43*, 181-188.

(13) Tao, X.; Liu, J.; Koley, G.; Li, X. B/SiO_x Nanonecklace Reinforced Nanocomposites by Unique Mechanical Interlocking Mechanism. *Adv. Mater.* **2008**, *20*, 1-6.

(14) Diao, H.; Robinson, P.; Wisnom, M.R.; Bismarck, A. Unidirectional Carbon Fibre Reinforced Polyamide-12 Composites with Enhanced Strain to Tensile Failure by Introducing Fibre Waviness. *Composites, Part A* **2016**, *87*, 186-193.

(15) Cheng, C.F.; Tsui, Y.C.; Clyne, T.W. Application of a Three-dimensional Heat Flow Model to Treat Laser Drilling of Carbon Fibre Composites. *Acta Mater.* **1998**, *46*, 4273-4285.

(16) Voisey, K.T.; Fouquet, S.; Roy, D.; Clyne, T.W. Fibre Swelling During Laser Drilling of Carbon Fibre Composites. *Opt. Lasers Eng.* **2006**, *44*, 1185-1197.

(17) Romoli, L.; Fischer, F.; Kling, R. A Study on UV Laser Drilling of PEEK Reinforced with Carbon Fibres. *Opt. Lasers Eng.* **2012**, *50*, 449-457.

(18) Riveiro, A.; Quintero, F.; Lusquiños, F.; del Val, J.; Comesaña, R.; Boutinguiza, M.; Pou, J. Experimental Study on the CO_2 Laser Cutting of Carbon Fibre Reinforced Plastic Composite. *Composites, Part A* **2012**, *43*, 1400-1409.

(19) Finger, J.; Weinand, M; Wortmann, D. Ablation and Cutting of Carbon-fibre Reinforced Plastics using Picosecond Pulsed Laser Radiation with High Average Power. *J. Laser Appl.* **2013**, *25*, 042007.

(20) O'Driscoll, D.; Hardwick, J.; Young, T.; Ryan, J. Lightning Strike of Perforated Carbon Fibre Epoxy Laminar Flow Panels. *J. Compos. Technol. Res.* **2000**, *22*, 71-76.

(21) Salama, A; Li, L; Mativenga, P; Sabli, A. High-power Picosecond Laser Drilling/machining of Carbon Fibre-reinforced Polymer (CFRP) Composites. *Appl. Phys. A: Mater. Sci. Process.* **2016**, *122*, 1-11.

(22) Ford, R.A. Thermo-ductile Composites: New Materials for 21st Century Manufacturing - Micro-perforation Symmetry. *Mater. Des.* **2002**, *23*, 431-439.

(23) Matthams, T.J.; Clyne, T.W. Mechanical Properties of Long-fibre Thermoplastic Composites with Laser Drilled Microperforations 1. Effect of Perforations in Consolidated Material. *Compos. Sci. Technol.* **1999**, *59*, 1169-1180.

(24) Matthams, T.J.; Clyne, T.W. Mechanical Properties of Long-fibre Thermoplastic Composites with Laser Drilled Perforations 2. Effect of Prior Plastic Strain. *Compos. Sci. Technol.* **1999**, *59*, 1181-1187.

(25) Dresselhaus, M.S.; Dresselhaus, G.; Saito, R.; Jorio, A. Raman Spectroscopy of Carbon Nanotubes. *Phys. Rep.* **2005**, *409*, 47-99.

(26) Hampe, A.; Kalinka, G.; Meretz, S.; Schulz, E. An Advanced Equipment for Single-fibre Pull-out Test Designed to Monitor the Fracture Process. *Composites* **1995**, *26*, 40-46.

(27) Jackson, A.P.; Vincent, J.F.V.; Turner, R.M. The Mechanical Design of Nacre. *Proc. R. Soc. B* **1988**, *234*, 415-440.

(28) Gao, H.; Ji, B.; Jager, I.L.; Arzt, E.; Fratzl, P. Materials Become Insensitive to Flaws at Nanoscale: Lessons from Nature. *Proc. Natl. Acad. Sci. U. S. A.* **2003**, *100*, 5597-5600.

(29) Checa, A.G.; Cartwright, J.H.E.; Willinger, M-G. Mineral Bridges in Nacre. *J. Struct. Biol.* **2011**, *176*, 330-339.

(30) Shao, Y.; Zhao, H-P.; Feng, X-I. Optimal Characteristic Nanosizes of Mineral Bridges in Mollusc Nacre. *RSC Adv.* **2014**, *4*, 32451-32456.

Acknowledgements

Stephen A. Hodge is greatly acknowledged for his help obtaining Raman spectra and mapping. The authors kindly acknowledge the funding for this research provided by EPSRC programme Grant EP/I02946X/1 on High Performance Ductile Composite Technology (HiPerDuCT), in collaboration with the University of Bristol. Prof. Amin Abdolvand acknowldges the support of EPSRC Career Acceleration Fellowship at the University of Dundee (EP/I004173/1).

Figure Captions

Figure 1. Schematic depicting (A) laser induced shape modification of carbon fibers (CF) mounted in card grids/frames from which (B) single frames containing fibers were cut, (C) Single fiber tensile tests were carried out after morphology characterization. SEM example of an expanded region after laser treatment, laser path highlighted red, altered morphology shown within the dashed red box. Designated fiber types detailed in box, SEM of irradiated carbon fiber samples illustrating the different observed morphologies before/after treatment, dependent on the experimental variables, average power, repetition rate and beam scanning speeds. Schematic shown adjacent shows average dimensions for Control, Expanded, Expanded/Ablated and Cotton-bud end fibers. Top right, distribution plot of maximum Expanded fiber diameters as a function of affected length deviating from as-received diameter (Control).

Figure 2. Tensile mechanical properties of (a) force to failure, (b) strength, (c) strain, and (d) modulus for Expanded and Expanded/Ablated fibers, relative to Control carbon fibers, as function of fiber expansion. Both force to failure and strength (normalised to control fiber diameter) are presented as the diameter at break of the failed laser treated fibers could not be ascertained.

Figure 3. Representative SEM image of an expanded fibers post tensile failure, demonstrating that the fibers failed near the thickest region.

Figure 4. Raman spectroscopy of fibers (Control, Expanded and Expanded/Ablated carbon fibers) along the fiber axis and at the fracture surfaces. (a) Schematic illustrating the relative position of (b) Raman spectra, Regions 1 to 5 on fiber surface,

with spectra separated by at least 20 μm, (c) Schematic cartoon Raman line-of-sight for fracture surfaces of (d) SEM, optical with schematic inset to describe the relative positions of (e) Regions A to E for the respective Raman graphs at the fracture surface. (f) Raman mapping of the fracture surfaces with relative intensity of G mode, and corresponding I_D/I_G and I_{2D}/I_G ratio shown as Raman maps within the range of 0.5 and 1.5 (colour image found on-line). N.B. Expanded and Expanded/Ablated fibers were irradiated in the B-C-D face in the relative fracture surfaces.

Figure 5. Optical micrograph series comparing the pull-out behaviour of (a) Control carbon fiber compared with (b) Cotton-bud end carbon fiber. Note that the field of view was adjusted during the series to follow the fiber end, all images have been positioned such that embedded position is maintained (blue dotted line), fiber ends are highlighted with an arrow where appropriate. Representative load-displacement plots of the pull-out behaviour of (c) Control carbon fiber and Cotton-bud end carbon fiber, with inset of average values of the interfacial shear strength (τ_{IFSS}) and work of pull-out.

FIGURES:

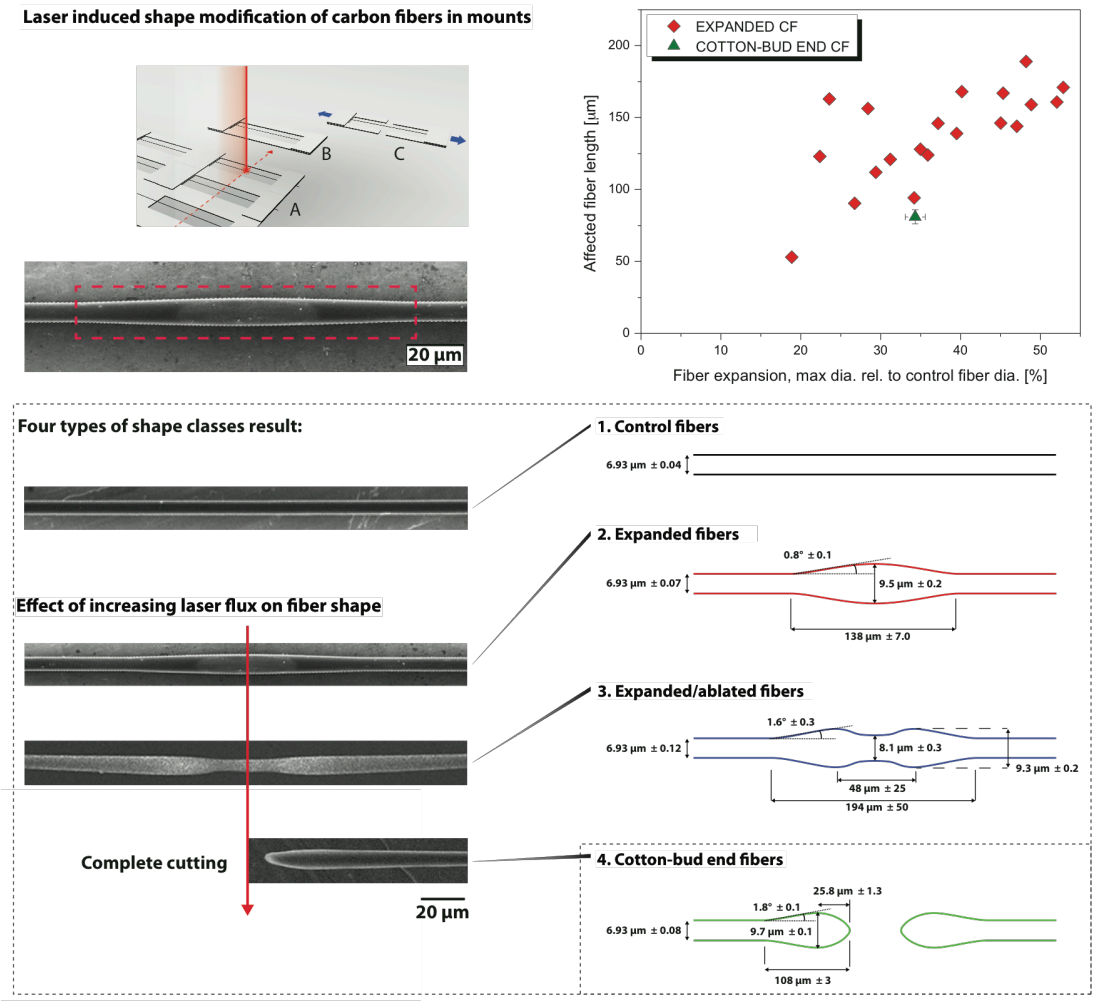

Figure 1.

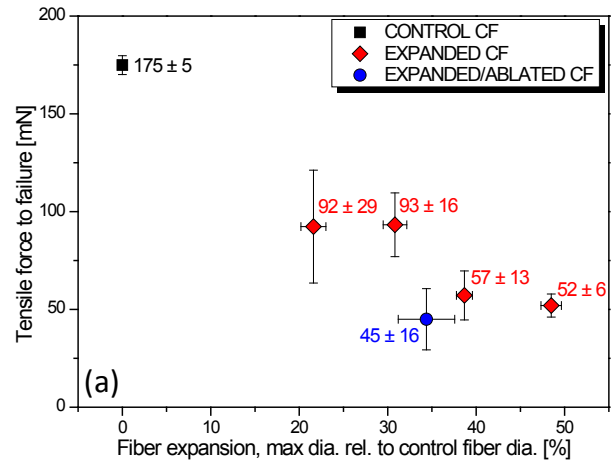
CONTROL CF
EXPANDED CF
EXPANDED/ABLATED CF
175 ± 5
92 ± 29
93 ± 16
57 ± 13
52 ± 6
45 ± 16
(a)
Tensile force to failure [mN]
Fiber expansion, max dia. rel. to control fiber dia. [%]

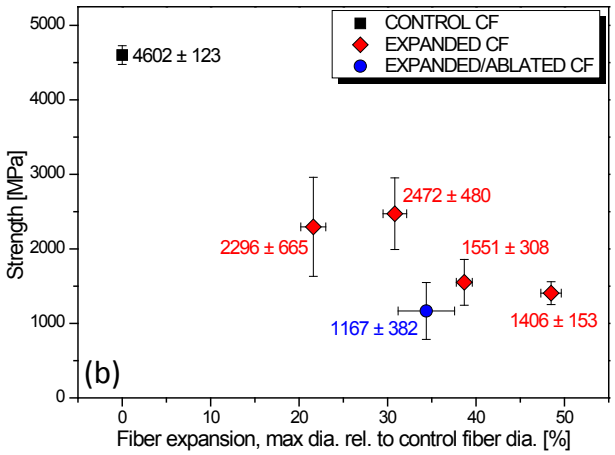
CONTROL CF
EXPANDED CF
EXPANDED/ABLATED CF
4602 ± 123
2472 ± 480
2296 ± 665
1551 ± 308
1406 ± 153
1167 ± 382
(b)
Strength [MPa]
Fiber expansion, max dia. rel. to control fiber dia. [%]

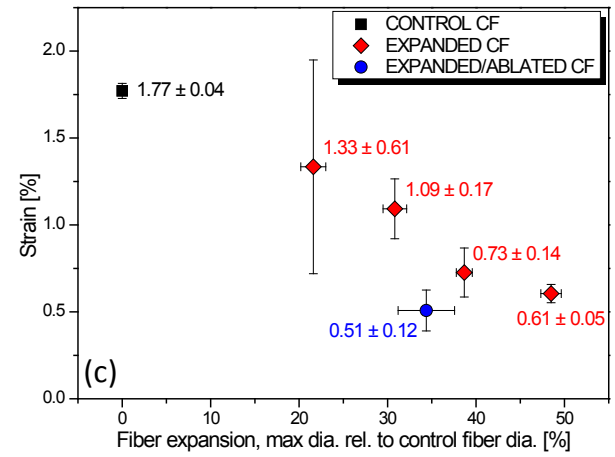
CONTROL CF
EXPANDED CF
EXPANDED/ABLATED CF
1.77 ± 0.04
1.33 ± 0.61
1.09 ± 0.17
0.73 ± 0.14
0.61 ± 0.05
0.51 ± 0.12
(c)
Strain [%]
Fiber expansion, max dia. rel. to control fiber dia. [%]

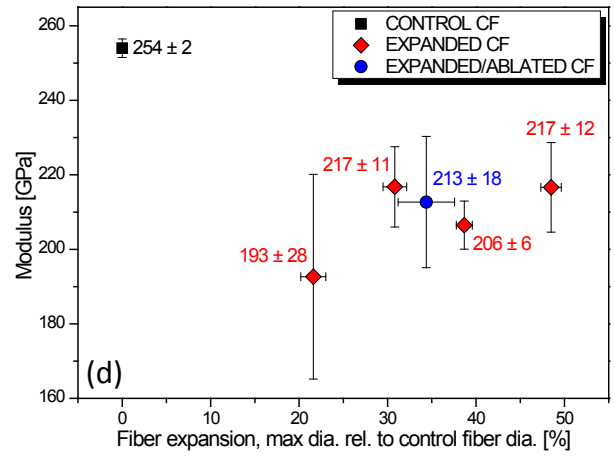
CONTROL CF
EXPANDED CF
EXPANDED/ABLATED CF
254 ± 2
217 ± 12
217 ± 11
213 ± 18
206 ± 6
193 ± 28
(d)
Modulus [GPa]
Fiber expansion, max dia. rel. to control fiber dia. [%]

Figure 2.

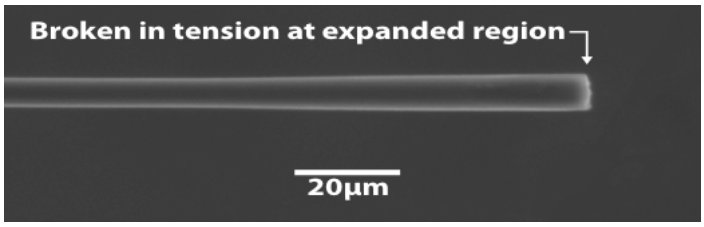

Figure 3.

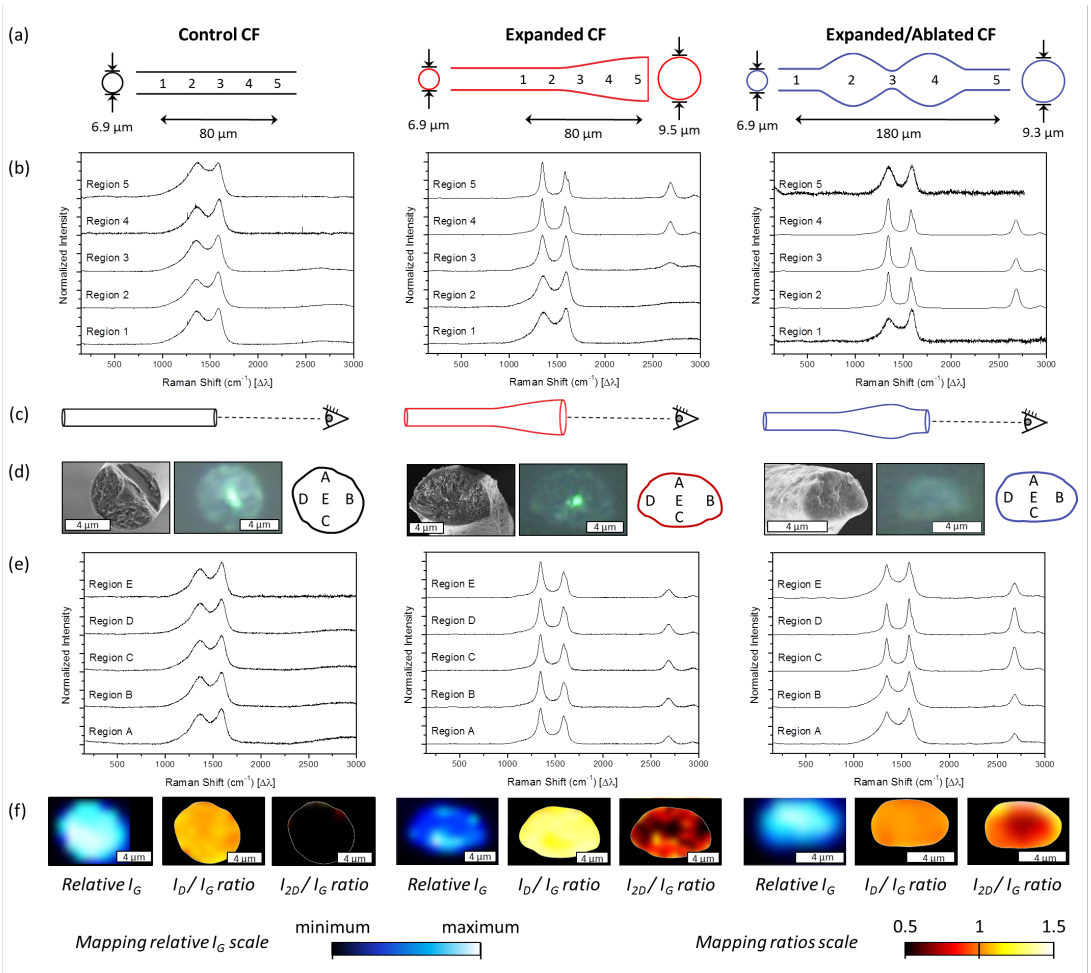

Figure 4.

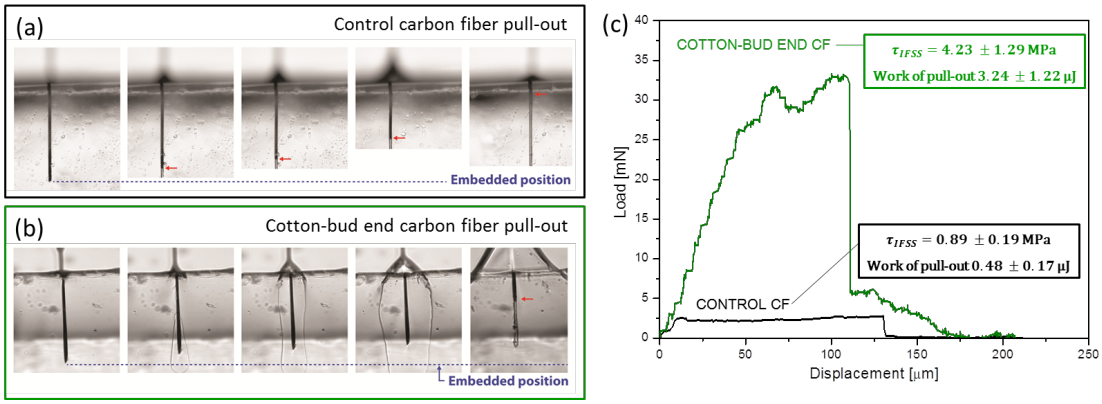

Figure 5.

TABLE OF CONTENTS GRAPHIC